

# Free-electron-laser-type interaction at 1 meter wavelength range

R. Drori, E. Jerby\*

Department of Electrical Engineering – Physical Electronics, Faculty of Engineering, Tel-Aviv University, Tel-Aviv 69978, Israel

## Abstract

A free-electron-laser (FEL)-type interaction is observed between a low-energy electron beam ( $\sim 0.7$  keV) and a radio wave in the VHF range ( $\lambda = 1.1$  m). The experimental device consists of a transmission-line (TEM-mode) cavity, and a folded-foil planar wiggler ( $\lambda_w = 4$  cm). Coherent oscillations are observed in the fundamental-cavity mode (0.28 GHz) and in higher-order modes. The FEL-type mechanism is demonstrated here in a new regime,  $\lambda \gg \lambda_w$ .

**Keywords:** Free-electron laser; Free-electron maser; VHF; UHF; radio waves

Free-electron lasers (FELs) [1] have been studied in the last decades in a wide spectrum of wavelengths. Various FELs have been demonstrated in the infrared [2], visible [3] and ultraviolet [4] ranges, as well as microwaves [5] and millimeter waves [6]. Our work [7] extends the operating range of the FEL-type interaction toward radio wavelengths and extremely low electron energies.

A typical FEL employs a relativistic e beam, which undulates in a periodic static magnetic field (wiggler) and interacts with an em wave. The synchronism condition for an FEL interaction with a tenuous e beam is

$$\omega \cong \frac{V_{ez}k_w}{1 \mp V_{ez}/V_{ph}}, \quad (1)$$

where  $V_{ez} = \beta_{ez}c$  is the average axial electron velocity,  $\omega$  and  $V_{ph}$  are the em wave angular frequency and phase velocity, respectively,  $k_w = 2\pi/\lambda_w$  is the wiggler periodicity, and the  $\mp$  sign denotes forward (–) and backward (+) em waves. The electron wiggling frequency is  $\omega_w = V_{ez}k_w$ . The term  $1 - V_{ez}/V_{ph}$  describes the Doppler up-shift effect. Space-charge effects and energy spread [8] may vary the FEL tuning relation (1).

Short wavelength FELs [2–4] operate with relativistic e beams in free-space ( $V_{ez} \rightarrow c$ ,  $V_{ph} = c$ ). Consequently, their Doppler frequency up-shift is large ( $\omega \gg \omega_w$ ). Free-electron masers (FEMs) [5,6] operate with mildly relativistic e beams in microwave and millimeter wave regimes. They employ hollow metallic waveguides ( $V_{ph} > c$ ), which reduce the Doppler shift term in Eq. (1) near cutoff.

Our FEL-type experiment operates in an extremely long wavelength ( $\lambda \sim 1$  m) and a low electron energy (down to 0.5 keV). This energy level is much lower than that of any

Table 1  
Operating regimes of FEL-type devices

Device	E-energy	Wavelengths	Em guide	$\lambda$ vs. $\lambda_w$
FEL	Relativistic	Microns	Free space	$\lambda \ll \lambda_w$
FEM	Mildly relativ.	Millimeters	Waveguide	$\lambda \sim \lambda_w$
FER	Non-relativistic	Meters	Transmission line	$\lambda \gg \lambda_w$

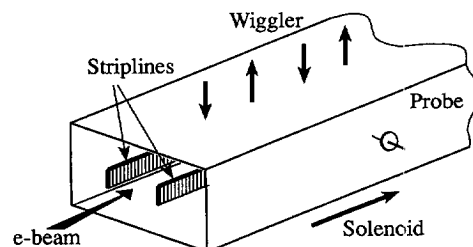


Fig. 1. A scheme of the experimental FER device.

known FEM experiment [9]. The device employs a non-dispersive transmission line which supports TEM modes. Hence,  $V_{ph} = c$  as in short-wavelength free-space FELs. The e beam in this experiment is extremely slow ( $V_{ez} \sim 0.05c$ ) and the Doppler shift is negligible. The FEL tuning condition (1) is reduced to  $\omega \sim \omega_w$  and, consequently,

$$\lambda \sim \lambda_w/\beta_{ez}. \quad (2)$$

The em wavelength is much longer here than the wiggler period ( $\lambda \gg \lambda_w$ ), and it reaches the VHF radio band. Therefore, the acronym FER is proposed here for this device. The main characteristics of the FEL, FEM and FER are summarized in Table 1.

The experimental FER device is illustrated in Fig. 1, and its parameters are listed in Table 2. The low-energy e beam is

\* Corresponding author. Fax: + 972 3 6423508; e-mail: jerby@taunivm.tau.ac.il.

Table 2  
Experimental parameters

Electron current	$\sim 0.1$ A at 1 keV
Pulse width	1–2 ms
Wiggler period	4.0 cm
Wiggler field	$\sim 0.4$ kG
Solenoid field	1–2 kG
Rectangular waveguide	$1.87 \times 0.87$ in. <sup>2</sup>
Distance between striplines	10.2 mm
Cavity length	53 cm
Quality factor	$4 \times 10^2$
Oscillation frequencies	0.28 GHz at 0.75 keV 0.56 GHz at 2.5 keV 0.85 GHz at 5.7 keV

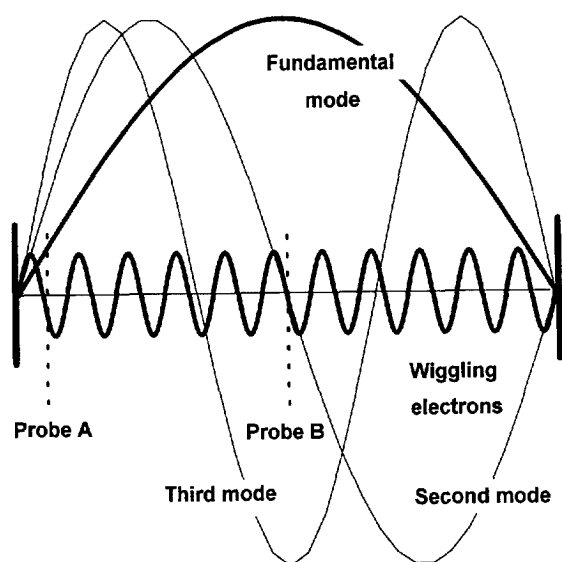


Fig. 2. The FER scaling ( $\lambda \gg \lambda_w$ ); the first three cavity modes with respect to the electron wiggling motion, and the positions of the RF probes.

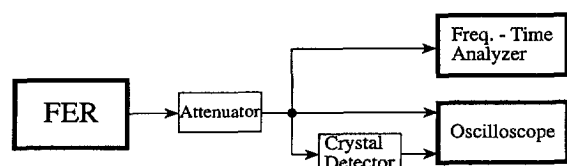


Fig. 3. The RF diagnostic scheme.

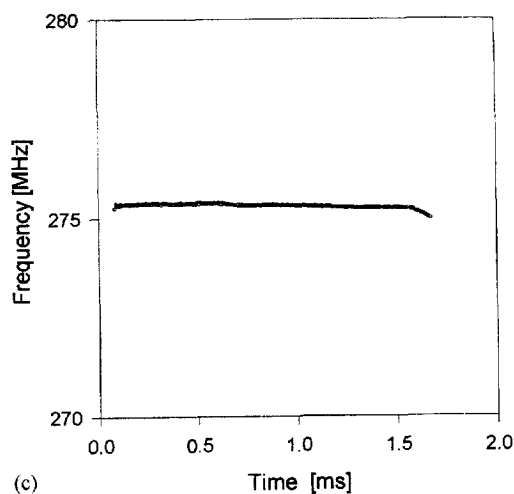
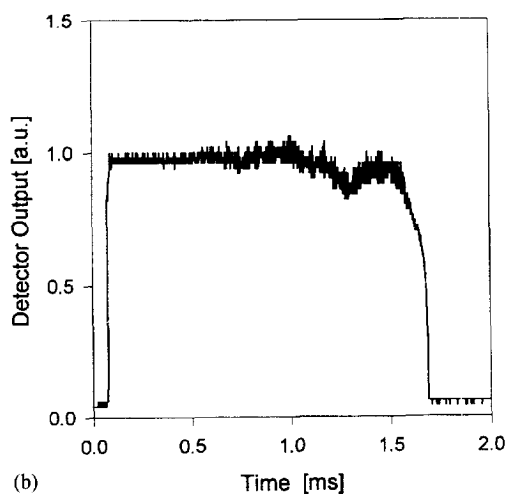
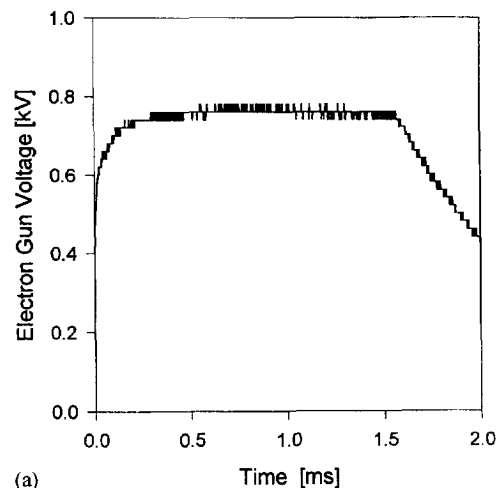


Fig. 4. The FER operation at the fundamental cavity mode; the e-gun voltage (a), the RF detector output (b), and frequency versus time measurements (c).

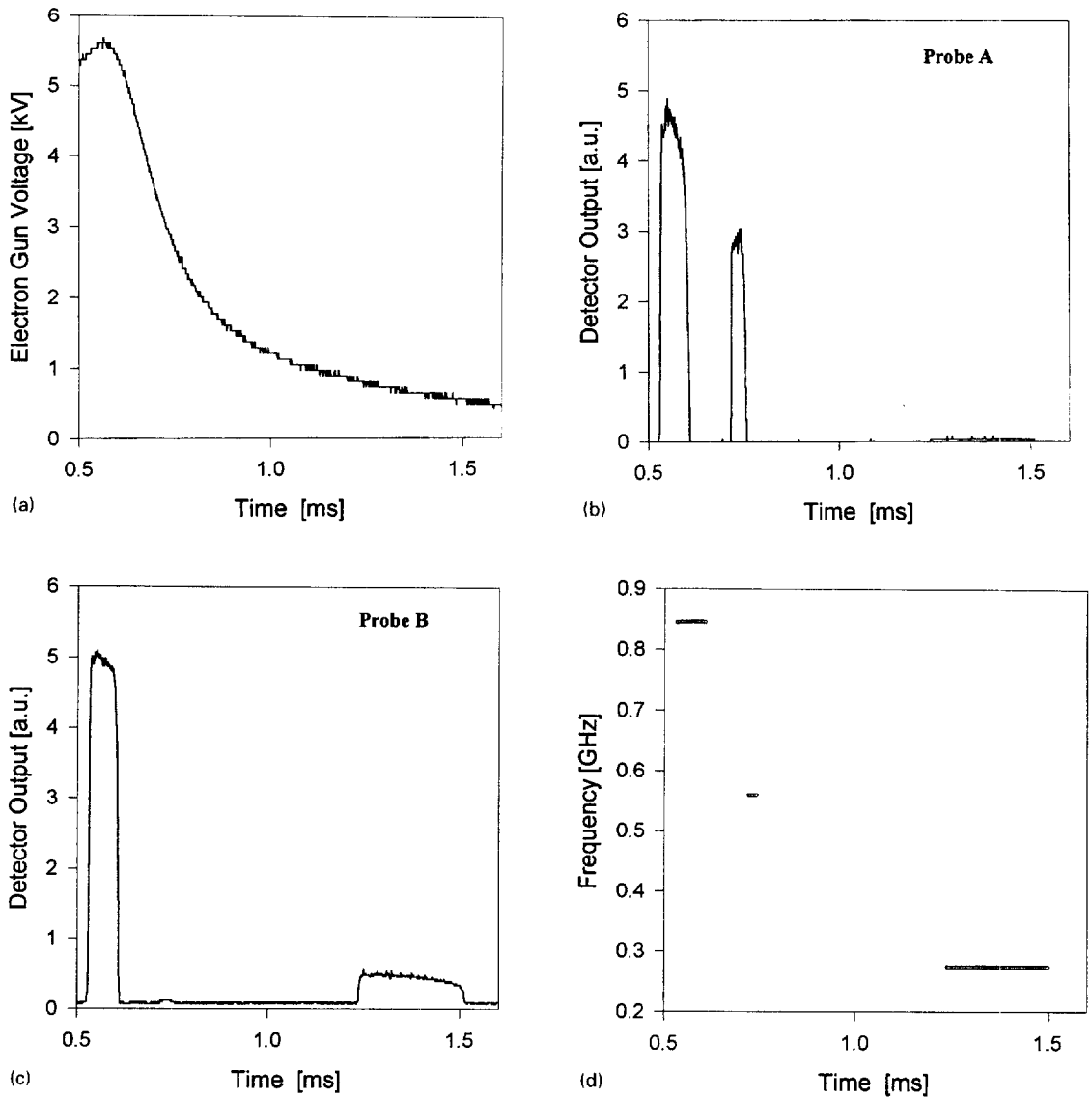


Fig. 5. The FER operation at the first three cavity modes; the e-gun voltage sweep (a), the RF detector outputs sampled by Probe A (b) and Probe B (c), and frequency versus time measurements (d).

generated by a planar thermionic cathode. A five-layer coaxially fed folded-foil [10] forms a planar wiggler ( $\lambda_w = 4$  cm) tapered at both ends. The e beam is confined by an axial magnetic field. Two parallel striplines stretched along a rectangular waveguide (WR187) provide a non-dispersive transmission line. Two mirrors with holes at both ends of the 53 cm long transmission line form a cavity (the mirror reactance slightly modifies the effective cavity length). The output signal is sampled by two dipole probes inserted into the narrow waveguide wall as illustrated in Fig. 1. Probe A is located 3 cm from the cavity mirror. Probe B is installed in the middle of the cavity's length, thus it samples only

the odd longitudinal modes. The different locations of the probes enable a distinction between the longitudinal cavity modes, as shown in Fig. 2.

Fig. 3 shows schematically the RF diagnostic set-up. The em power evolved in the cavity is sampled by the RF probes, attenuated, and split for amplitude and frequency measurements. The signals are detected by calibrated crystal detectors (Elisra-MW-1170D, HP-8474D). The low operating frequency enables a direct observation of the FER output signals by a fast digital oscilloscope (without any envelope-detection or mixing). In addition, a frequency and time interval analyzer (HP-5372A) is

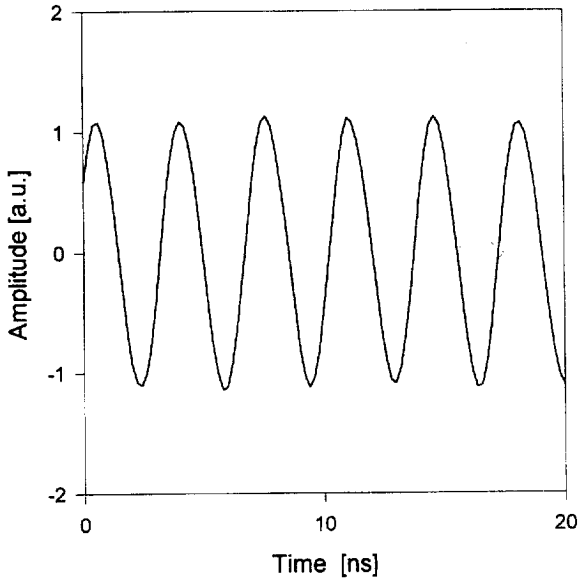


Fig. 6. A direct oscilloscope observation of the fundamental FER mode oscillation.

used to measure the signal-frequency evolution during the pulse.

The FER experimental results are presented in Figs. 4–7. The interaction with the fundamental longitudinal mode of the cavity is demonstrated in Figs. 4(a)–(c). The e-gun voltage pulse shown in Fig. 4(a) has a maximum voltage of 760 V (unregulated) and a pulse width of  $\sim 2$  ms. The detector output of the corresponding RF signal is shown in Fig. 4(b). Its spectral evolution is measured by the frequency and time-interval analyzer as shown in Fig. 4(c). A coherent oscillation at 275 MHz ( $\lambda = 109$  cm) is clearly observed. This frequency corresponds to the fundamental longitudinal mode of the cavity.

A sweep in the e-gun voltage as shown in Fig. 5(a) yields a sequence of oscillations in the first three longitudinal modes. The simultaneous detector outputs of Probes A and B are shown in Figs. 5(b) and (c), respectively. The measured frequencies of the three pulses shown in Fig. 5(d), are 0.85, 0.55 and 0.28 GHz, in agreement with the third, second, and first longitudinal cavity modes, respectively. The mode identification is confirmed by the coupling of the second mode to Probe A and not to Probe B (located in a null of the even modes). In addition, the fundamental mode coupling to Probe B is larger than to Probe A, in accordance with their different locations. Fig. 6 shows a direct oscilloscope measurement of the FER oscillation at the fundamental mode.

An accumulation of over one hundred experimental shots is presented in the form of a frequency–voltage map in Fig. 7. Each dot represents the measured frequency and e-gun voltage at the peak of each RF pulse. Three groups of dots are clearly observed in the frequencies of the first three longitudinal modes listed in Table 2. The curved line in Fig. 7

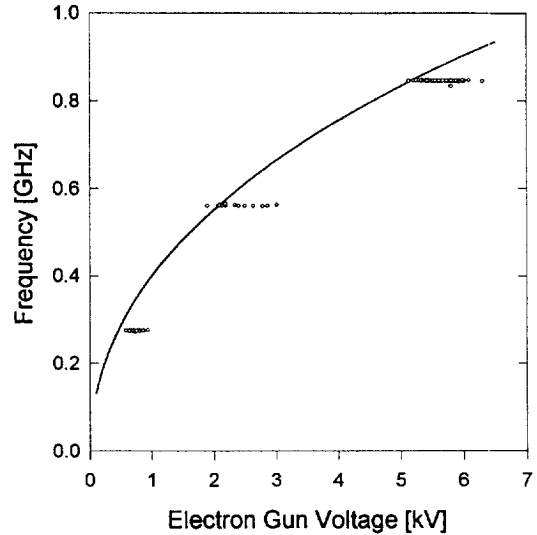


Fig. 7. A frequency–voltage diagram of the FER device; experimental results (dots) and the theoretical FEL tuning curve (1).

shows the theoretical FEL tuning relation (1) for a backward wave. The slightly higher gun voltages in the experimental results are attributed to small space-charge effects. The voltage spread in each mode reflects the detuning acceptance [8].

In conclusion, the experiment presented in this paper extends the proven operating range of the FEL-type interaction towards the long wavelength limit. The new operating regime,  $\lambda \gg \lambda_w$ , is associated with an FEL operation in extremely low e-gun voltages (below 1 kV in our experiment). Coherent oscillations are clearly observed in several cavity modes. The ability of a direct oscilloscope observation may provide a clear insight into FEL time-domain phenomena. In practice, low-voltage FER devices might be considered for long-wavelength communication and industrial applications.

This work was partially supported by the Israeli Ministries of Energy and Science, the Belfer Center for Energy Research, and the Israeli Academy of Science and Humanities.

## References

- [1] H.P. Freund, T.M. Antonsen, *Principles of Free-electron Lasers*, Chapman & Hall, London, 1992, and references therein.
- [2] L.R. Elias, W.M. Fairbank, M.J. Madey, H.A. Schwettman, T.I. Smith, *Phys. Rev. Lett.* 36 (1976) 717.
- [3] M. Billardon, P. Ellaume, J.M. Ortega, C. Bazin, M. Bergher, M. Velghe, Y. Petroff, *Phys. Rev. Lett.* 51 (1983) 1652.

- [4] G.N. Kuliapanov, V.N. Litvinenko, I.V. Panaev, V.M. Popik, A.N. Skrinsky, A.S. Sokolov, A.N. Vinokurov, *Nucl. Instr. and Meth. A* 296 (1990) 1.
- [5] R.M. Phillips, *Nucl. Instr. and Meth. A* 272 (1988) 1.
- [6] T.J. Orzechowski, B.R. Anderson, J.C. Clark, W.M. Fawley, A.C. Paul, D. Prosnitz, E.T. Scharlemann, S.M. Yarema, D.B. Hopkins, A.M. Sessler, J.S. Wurtele, *Phys. Rev. Lett.* 57 (1986) 2172.
- [7] R. Drori, E. Jerby, A. Shahadi, *Nucl. Instr. and Meth. A* 358 (1995) 151.
- [8] E. Jerby, A. Gover, *IEEE J. Quantum Electron.* QE-21 (1985) 1041.
- [9] H.P. Freund, V.L. Granatstein, *Nucl. Instr. and Meth. A* 358 (1995) 551.
- [10] A. Sneh, E. Jerby, *Nucl. Instr. and Meth. A* 285 (1989) 294.